

Reconstructed rheometer for direct monitoring of dewatering performance and torque in tailings thickening process

Yong Wang, Ai-xiang Wu, Zhu-en Ruan, Zhi-hui Wang, Zong-su Wei, Gang-feng Yang, and Yi-ming Wang

Cite this article as:

Yong Wang, Ai-xiang Wu, Zhu-en Ruan, Zhi-hui Wang, Zong-su Wei, Gang-feng Yang, and Yi-ming Wang, Reconstructed rheometer for direct monitoring of dewatering performance and torque in tailings thickening process, *Int. J. Miner. Metall. Mater.*, 27(2020), No. 11, pp. 1430-1437. <https://doi.org/10.1007/s12613-020-2116-y>

View the article online at [SpringerLink](#) or [IJMMM Webpage](#).

Articles you may be interested in

Di Liu, Min-jie Lian, Cai-wu Lu, and Wen Zhang, [Effect of the lenticles on moisture migration in capillary zone of tailings dam](#), *Int. J. Miner. Metall. Mater.*, 27(2020), No. 8, pp. 1036-1045. <https://doi.org/10.1007/s12613-020-1963-x>

Xiao-dong Hao, Yi-li Liang, Hua-qun Yin, Hong-wei Liu, Wei-min Zeng, and Xue-duan Liu, [Thin-layer heap bioleaching of copper flotation tailings containing high levels of fine grains and microbial community succession analysis](#), *Int. J. Miner. Metall. Mater.*, 24(2017), No. 4, pp. 360-368. <https://doi.org/10.1007/s12613-017-1415-4>

Rui-min Jiao, Peng Xing, Cheng-yan Wang, Bao-zhong Ma, and Yong-Qiang Chen, [Recovery of iron from copper tailings via low-temperature direct reduction and magnetic separation: process optimization and mineralogical study](#), *Int. J. Miner. Metall. Mater.*, 24(2017), No. 9, pp. 974-982. <https://doi.org/10.1007/s12613-017-1485-3>

Shi Wang, Xue-peng Song, Xiao-jun Wang, Qiu-song Chen, Jian-chun Qin, and Yu-xian Ke, [Influence of coarse tailings on flocculation settlement](#), *Int. J. Miner. Metall. Mater.*, 27(2020), No. 8, pp. 1065-1074. <https://doi.org/10.1007/s12613-019-1948-9>

Peng Li, Yun-bing Hou, and Mei-feng Cai, [Factors influencing the pumpability of unclassified tailings slurry and its interval division](#), *Int. J. Miner. Metall. Mater.*, 26(2019), No. 4, pp. 417-429. <https://doi.org/10.1007/s12613-019-1750-8>

Jalil Pazhoohan, Hossein Beiki, and Morteza Esfandyari, [Experimental investigation and adaptive neural fuzzy inference system prediction of copper recovery from flotation tailings by acid leaching in a batch agitated tank](#), *Int. J. Miner. Metall. Mater.*, 26(2019), No. 5, pp. 538-546. <https://doi.org/10.1007/s12613-019-1762-4>



IJMMM WeChat



QQ author group

Reconstructed rheometer for direct monitoring of dewatering performance and torque in tailings thickening process

Yong Wang¹⁾, Ai-xiang Wu^{1,2)}, Zhu-en Ruan¹⁾, Zhi-hui Wang¹⁾, Zong-su Wei³⁾, Gang-feng Yang¹⁾,
and Yi-ming Wang¹⁾

1) School of Civil and Resource Engineering, University of Science and Technology Beijing, Beijing 100083, China

2) Key Laboratory of the Ministry of Education of China for High-Efficient Mining and Safety of Metal Mines, University of Science and Technology Beijing, Beijing 100083, China

3) Section for Biological and Chemical Engineering, Department of Engineering, Aarhus University, Høngøvej 2, DK-8200, Aarhus N, Denmark

(Received: 29 March 2020; revised: 14 May 2020; accepted: 8 June 2020)

Abstract: To further clarify the dewatering performance and torque evolution during the tailings thickening process, a self-made rake was connected to a rheometer to monitor the shear stress and torque. The dewatering performance of the total tailings was greatly improved to a solid mass fraction of 75.33% in 240 min. The dewatering process could be divided into three stages: the rapid torque growth period, damping torque growth period, and constant torque thickening zone. The machine restart was found to have a significant effect on the rake torque; it could result in rake blockage. Furthermore, the simultaneous evolution of the torque and solid mass fraction of thickened tailings was analyzed. A relationship between the torque and the solid mass fraction was established, which followed a power function. Both the experimental and theoretical results provide a reference for the deep cone thickener design and operation to enhance the dewatering performance.

Keywords: tailings; dewatering; rake; reconstructed rheometer; torque monitoring

1. Introduction

Owing to the development in paste technology, huge amounts of total tailings can be dewatered, thickened into paste slurry, and then transported to underground stopes or surfaces for disposal [1–4]. With paste technology, the solid waste (tailings) is well managed, and spent water is effectively recovered [5–7], affording the advantages of safety, eco-friendliness, cost-effectiveness, and efficiency [8–10]. Since total tailings are too fine to be dewatered and thickened [11], the conventional gravity high-rate thickener and filter, in addition to being costly, will result in a low solid mass fraction of underflow. Compared with other thickeners, the deep cone thickener (DCT) is the optimal choice for paste technology [12].

To obtain appropriate underflow using the DCT, many researchers have studied the influence of the flocculant and rake using both experiments and simulations. The research topic has transitioned from gravity sedimentation and static thickening to flocculation sedimentation and dynamic thickening [13]. Using a suitable flocculant type and dosage,

which results in good coagulation and flocculation of total tailings, is conducive to rapid sedimentation and dewatering [4, 14–16]. Moreover, the feedwell of the DCT is essential for flocculation [17]. The structure of the feedwell is optimized through computational fluid dynamics (CFD) simulation, and then the feed solid mass fraction and rate, flocculant dosage, and flocculant addition location can be optimized and determined [18–20].

Furthermore, the rake, which transports the sediment from the tank bottom to the underflow discharge orifice, is another essential part of the DCT [21]. Through dynamic thickening experiments and CFD simulation, several studies on the rake have concentrated on its influence on the dewatering behavior, the rake torque calculation, and the rake design. Wu *et al.* [22] conducted a laboratory experiment to explore the effect of the rake rod number and rake rod arrangement on the dewatering behavior of copper mine tailings and proposed a torque model for a complex-structure rake. Du *et al.* [23] studied the impact of rake on the aggregate structure, proving the existence of “drainage channel” as a result of raking, which contributes to the movement of water from the bottom

to the top of the DCT. White *et al.* [19] investigated the flow patterns around the rake with CFD modeling. Huang *et al.* [24] and Ruan *et al.* [25] simulated the influence of the raking speed and rake structure on the dewatering.

The rake torque is a key parameter in the DCT operation and is mainly influenced by the yield stress of the suspension [26–27]. In general, the underflow produced by the DCT has a yield stress of over 100 Pa, which is much higher than those of the underflow produced by the conventional high-rate thickeners (20–30 Pa) and high-density thickeners (30–100 Pa) [12]. Kahane *et al.* [28] derived the torque variation law of a thickener at Worsley Alumina Pty Ltd. with CFD modeling. Rudman *et al.* [29] investigated the influence of the yield stress of the suspension, rake rotational speed, and rake structure on the rake torque, providing guidance for rake design. Based on the DCT model dynamic settlement test and rheological parameters measurement, Li *et al.* [30] analyzed the rake blockage in a DCT. Wang *et al.* [31] proposed a torque mathematical model and predicted that the rake torque increased with an increase in solid mass fraction and bed height during the DCT operation. Tan *et al.* [32] derived a model of rake torque to control the solid mass fraction. Although much attention has been paid to the dynamic sedimentation considering the rake in DCTs, very few studies on rake torque monitoring, which is essential for the DCT design and operation in laboratory experiments, have been published.

The Chambishi Copper Mine (CCM) of NFC Africa Mining Plc, located in the central of the Copperbelt province, Zambia, Africa, has recently adopted the cemented paste backfill (CPB) system. Since the accurate prediction of the solid mass fraction of underflow is central to the CPB design, in this study, a rheometer was modified with a self-made rake and used to conduct laboratory experiments on the dynamic dewatering of total tailings from the CCM and monitor the rake torque. The results can provide guidance and reference for the DCT design and operation. In this way, we have not only overcome the lack of a dynamic dewatering experimental installation but also proposed a new approach for monitoring the shear stress and rake torque in the dewatering process.

2. Experimental

2.1. Materials

The true density of total tailings from the CCM was 2.77 g/cm³, and the corresponding bulk density was 1.46 g/cm³. The porosity was 47.29vol%. The true solid densities of the tailings were determined using Eq. (1), based on the specific gravity test results.

$$\rho_s = G_s \rho_w \quad (1)$$

where G_s is the specific gravity of dry tailings, ρ_s is the true solid density of dry tailings, and ρ_w is the density of water at 20°C, which is 998.23 g/cm³. The specific gravity (G_s) of the tailings was calculated following our previous study [31].

The cumulative particle distribution of the tailings was as follows: 36.39% were under 25 μm , 46.66% were under 38 μm , 64.50% were under 74 μm , and 17.08% were coarser than 0.18 mm. The particle size distribution of the total tailings samples was determined by artificial sieving methods, as shown in Fig. 1.

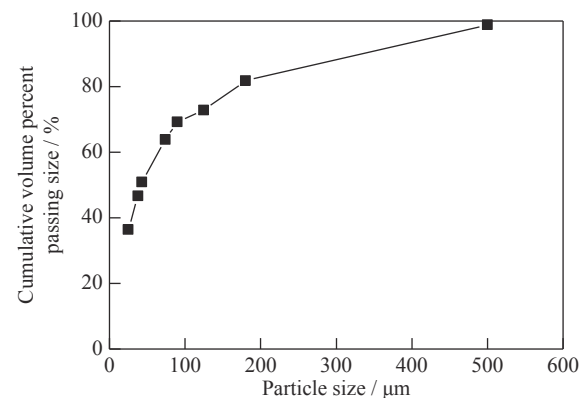


Fig. 1. Particle size distribution of total tailings.

The mineralogical analysis of the micronized tailings was carried out using X-ray fluorescence, the result of which is given in Table 1. The main chemical composition of the tailings sample was SiO₂, with a mass fraction of 47.82%.

Table 1. Chemical composition of the tailings

															wt%
SiO ₂	Al ₂ O ₃	CaO	MgO	K ₂ O	Na ₂ O	S	P	Cu	Co	Pb	Zn	Fe	Loss on ignition	Total	
47.82	9.71	11.5	8.89	4.51	0.2	0.35	0.06	0.1	0.03	0.02	0.02	1.94	9.38	94.53	

As determined from the flocculant selection experiment, Magnafloc 5250 from Badische Anilin-und-Soda-Fabrik (BASF), a German chemical company, was a suitable flocculant for the CCM tailings (rapid settling and a relatively low dosage). The optimal flocculant dosage was 20 g/t. The molecular weight of the flocculant was 13 million.

2.2. Reconstructed rheometer

A self-made dynamic dewatering device was reconstructed.

It was based on a Brookfield R/S Plus rheometer slow-speed rotating motor (Fig. 2). The device has an adjustable rotational speed (0.01–800 r/min) and can monitor parameters such as shear stress (0–2000 Pa), viscosity (0.001–80000 Pa·s), and torque (0.05–50 mN·m) during the mixing of tailings slurry. The torque resolution and angular resolution are 0.01 mN·m and 0.8 mrad, respectively. The accuracy of the device is $\pm 1\%$ of the maximum torque value.

The primary aim of this study was to establish a protocol

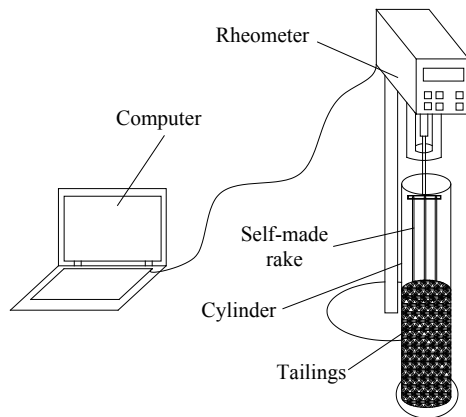


Fig. 2. Schematic of the operation of the rheometer-based dynamic thickening device.

to measure the solid mass fraction (i.e., dewatering performance) using a combination of experimental and theoretical tools. To this end, one rotation rate was set to attain such modeling prediction, although other rotation rates would lead to models serving the same purpose. The rotational speed in our experiments was selected considering the very low rake rotation of the DCT in engineering practices. While a high speed is prone to produce a larger torque value during the measurement, the low-speed measurement cycle could cause mud layer consolidation and a larger measurement torque value, all of which may cause a sudden stop of the rake. Therefore, an appropriate speed must be selected. We selected a low rotation speed of 5 r/min on the basis of the previous small-scale experimental study [33]. In this study, we employed a self-made rake and connected it with the rheometer. Since the shear stress and apparent viscosity tested by the self-made rake were not accurate, the torque tested in this study was used to predict the dewatering performance of tailings. Generally, for the case when a vane rotor rheometer is used, the conversion formula between the shear stress and torque is given as follows [30,34]:

$$\tau = \frac{T}{2\pi R^3 \left(\frac{H}{R} + \frac{2}{3} \right)} \quad (2)$$

where H and R are the height and radius dimensions of the paddle rotor, respectively; T and τ are torque and shear stress, respectively. The self-made rake is not paddle-shaped, so it is difficult to obtain the regular integral area and thus the shear stress from the measured torque value. Therefore, shear stress and shear rate are also used in this study. The torque value is accurate, while the shear stress value is the relative value that can reflect the evolution rule of shear stress.

2.3. Testing method

2.3.1. Ultimate solid mass fraction determination

The device was used for the dynamic thickening experiment. Before the experiment, the mass of the water per milli-

metre of the measuring cylinder was calculated; in the conversion, the rake needed to be placed in the measuring cylinder experiments given that the rake also occupied a certain volume. When the mass of the water was 1833.9 g, the corresponding height was 212 mm, and when the mass of the water was 1015.0 g, the corresponding height was 58 mm. The mass of water corresponding to 1 mm height was calculated to be 5.3175 g.

In the process of industrial dewatering by the DCT, the flocculant solution is continuously added to the feedwell to mix with the tailings slurry, almost without rest time in the metal mines. However, before the flocculant solution is pumped into the feedwell, it should be stirred for 1 to 2 h, depending on parameters, such as the molecular weight and temperature. In this study, before the flocculant solution was added to the cylinder, we stirred the flocculant solution using a jar tester at 200 r/min for 15 min and then at 125 r/min for 75 min. In addition, the flocculant solution was left for 1 d for maturation before use [35].

First, 1400 g of water was added to the measuring cylinder, and 16 g of a flocculant solution with a solid mass fraction of 0.1% was further added, and then the flocculant solution was stirred for 3 min. Then, 800 g of tailings was added. By recording the height of the mud layer at different times, one can calculate the corresponding solid mass fraction using the following formula:

$$C_w = \frac{m_1}{(m_1 + m_2) - (H_1 - H_2) \times 5.3175} \quad (3)$$

where C_w is the solid mass fraction; m_1 and m_2 are the mass of tailings and water, respectively; H_1 represents the scale corresponding to the clear water, and H_2 represents the scale corresponding to the mud layer interface.

2.3.2. Shear stress and torque monitoring

The experiment was conducted using 600 g of tailings, 1400 g of water, and 12 g of 0.1% flocculant solution. In the previous experiment, the ratio of the final mud layer height to cylinder diameter was obtained as 0.83:1, which is similar to the ratio of mud layer height to diameter of the existing DCTs in other similar mines. The two parameters of shear stress and torque were monitored from the feeding. According to the actual operation of the DCT, the shear stress and torque evolution were investigated under the following three aspects: (1) the effect of the feeding process on the shear stress and torque evolution; (2) the effect of the thickening time on the shear stress and torque evolution; (3) the effect of machine restart on the shear stress and torque evolution.

3. Results and discussion

3.1. Evolution of solid mass fraction of tailings suspension at various thickening times

According to Eq. (3), the solid mass fraction corresponding to different thickening times were calculated, as shown in

Fig. 3. It can be seen that the solid mass fraction increased rapidly at the beginning (60 min) and then remained stable at around 75% (>60 min); the limit dewatering solid mass fraction of the total tailings from the CCM was 75.33%. When the rake rotation speed was 0 r/min, the limit solid mass fraction could reach 66.29% after 48 h sedimentation when the same consumption flocculant was added. The average solid mass fraction of the slurry obtained by the dynamic experimental device was approximately 13.64% higher than that of the static sedimentation within the same measuring cylinder. Moreover, the evolution of solid mass fraction obtained by the reconstructed rheometer in this study is similar to those of our previous studies [36–38], which indicates that the reconstructed rheometer can be used to study the dewatering performance of thickened tailings. The solid mass fraction obtained by dynamic sedimentation was closer to the DCT underflow, and the solid mass fraction obtained by static sedimentation was closer to the solid mass fraction of underflow of the vertical sand tank without the rake.

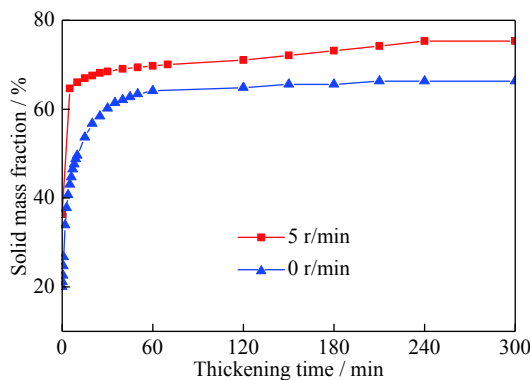


Fig. 3. Evolution of the solid mass fraction at different rotation speeds.

3.2. Evolution of shear stress and torque during the dynamic dewatering

Since the dynamic thickening device can monitor the shear stress and torque, which are two very important parameters during the thickening process, the shear stress and torque evolution was studied to provide a reference for the DCT operation and manipulation.

3.2.1. Effect of feeding process on shear stress and torque evolution

First, the flocculant was added while the solution was constantly being stirred. The tailings were added after 2 min of stirring. During the tailings addition (named as the feeding process, about 4 min), the shear stress and torque continuously increased. At the end of the feeding, the shear stress was 130 Pa and the torque was around 4 mN·m, which were respectively 1/6.3 and 1/6 of the shear stress and torque at smooth operation. The shear stress and torque changes dur-

ing the feeding process are illustrated in Fig. 4. Thus, it can be inferred that in the DCT, the torque also significantly increased during the initial feeding process.

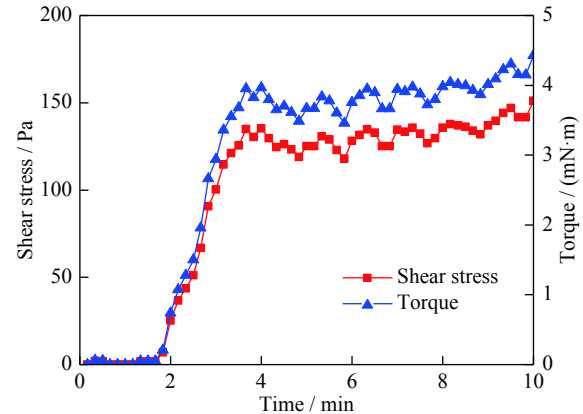


Fig. 4. Effect of feeding process (about 4 min) on the shear stress and torque of rake.

3.2.2. Effect of thickening time on shear stress and torque evolution

Under the action of the rake and gravity, the tailings continued to settle, and the pore water continued to rise along the water guiding channel opened by the rake. Owing to the continuous dehydration, the tailings slurry density kept growing. Therefore, the shear stress and torque increased continuously during the thickening process. The relationships between the shear stress and torque of 250 min in the thickening process are illustrated in Fig. 5. When the thickening time was increased to 120 min, the increase rates of the shear stress and torque were small and gradually became constant. This is because the concentrated tailings could not be dehydrated further at a certain dense porosity, so that the solid mass fraction of the tailings tended to be constant. However, during the first 120 min of dehydration, the solid mass fraction of the slurry in the container gradually increased (Fig. 3), which is the main cause of the increase in shear stress or torque. After 120 min, the rake shear stress or torque remained at a constant value. At the constant rake speed of 5 r/min, the apparent viscosity could be assumed to be constant (with the progression of the dehydration time, the slurry apparent viscosity basically remained unchanged, almost maintaining a finite value). Moreover, considering the viscosity bifurcation effect of flocculating tailings particles [39–40], the slurry in the equipment was in the low-speed flow area, rather than in the microstructure development region of the aging area (i.e., the increased viscosity area). Therefore, the increase in the rake shear stress or torque within the first 120 min of tailings slurry in the equipment was mainly due to the increase in the slurry solid mass fraction caused by dehydration. For the next 130 min, the solid mass fraction of the slurry was constant, probably due to the ceased dehydration effect; meanwhile, the rake shear stress and torque under a low rotation speed

also basically remained unchanged. In this case, the aging effect caused by the microstructure development in the slurry was not significant at a low rotation speed. Therefore, when the tailings descended to a certain extent, the shear stress and torque were largely constant.

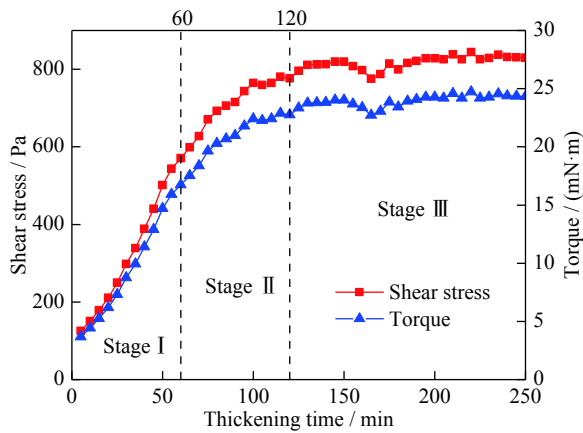


Fig. 5. Evolution law of shear stress and torque of rake in dense process.

The thickening process of the tailings can be divided into three stages according to the changes in shear stress and torque during the tailings thickening process: The first is the period of rapid torque growth, corresponding to the thickening time of 0–60 min; here, the shear stress and torque rapidly increased to 571 Pa and 17 mN·m, respectively. The second is the period of damping torque growth, corresponding to the thickening time of 60–120 min; here, the shear stress increased from 571 to 776 Pa, which is 1.36 times that of 60 min, and the torque increased from 17 to 23 mN·m, which is 1.35 times that of 60 min. The shear stress and torque still increased in this process, but the growth rates reduced significantly. The third is the dense period of constant torque, corresponding to the thickening time of >120 min; here, the shear stress and torque tended to be constant. For example, when the thickening time was 240 min, the shear stress and torque were 832 Pa and 24 mN·m, respectively, which were almost equal to the values at 120 min.

3.2.3. Effect of machine restart on shear stress and torque evolution

The DCT may suddenly stop running and then restart owing to unpredictable factors such as sudden equipment failure or power failure during production. Thus, the effect of shutdown and restart were considered. The shear stress and torque changes were studied in three cases of shutdown: a first shutdown for 5 min; a second shutdown for 30 min, and a third shutdown with immediate restart.

(1) Shutdown for 5 min.

After the thickening time exceeded 250 min, the thickening device was stopped, and after 5 min, it was restarted. The shear stress and torque variation are shown in Fig. 6. The ini-

tial shear stress and torque were 1000 Pa and 29 mN·m, respectively, which were 1.20 and 1.21 times those of the smooth operation before shutdown (at 240 min). After 2 min of restart, the shear stress and torque substantially returned to the value before the shutdown.

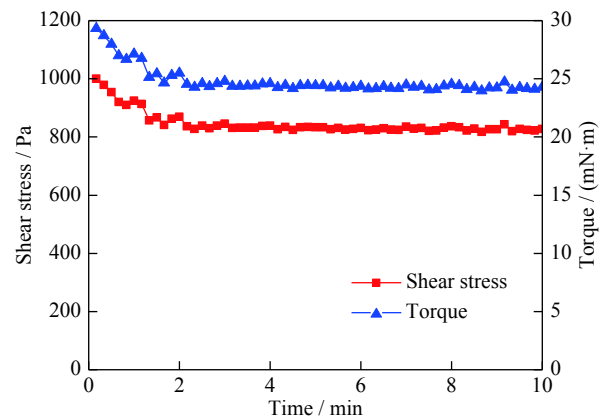


Fig. 6. Variation of shear stress and torque for the case of restart after 5 min shutdown.

(2) Shutdown for 30 min.

The thickening device was stopped again and then restarted after 30 min. Fig. 7 illustrates the variation of the shear stress and torque. The initial shear stress and torque were 1444 Pa and 42 mN·m, respectively, which were 1.74 and 1.75 times those of smooth operation before shutdown. The same as shutdown for 5 min, the shear stress and torque also substantially returned to the normal operating value after 2 min of restart.

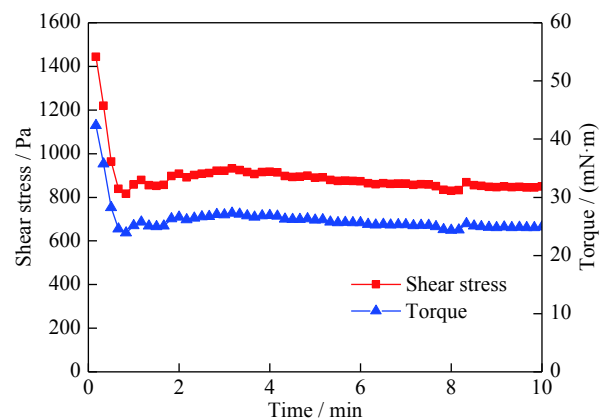


Fig. 7. Variation of shear stress and torque for the case of restart after 30 min shutdown.

(3) Immediate restart after shutdown.

The DCT was stopped a third time and restarted quickly (shutdown for 1 min). The shear stress was as high as 1865 Pa and the torque was 55 mN·m, which were 2.4 and 2.3 times the normal operating value. After one set of data was read, the rake stopped rotating. Two attempts to restart the

DCT were unsuccessful. As a result, the so-called rake blockage accident of the DCT had occurred. Therefore, when the DCT shuts down after a power failure, it is necessary to discharge the tailings in the deep cone as quickly as possible or restore the power supply as soon as possible to prevent the rake blockage accident.

3.3. Simultaneous evolution of solid mass fraction and torque at various thickening times

For tailings dewatering, the thickened solid mass fraction is one of the most important parameters. A high solid mass fraction of thickened tailings is desired for the tailings disposal (because of advantages such as high water recovery, reduced waste volume, and less heavy metal pollution). Therefore, the simultaneous evolution of the solid mass fraction and torque at various thickening times was studied, and the results are shown in Fig. 8.

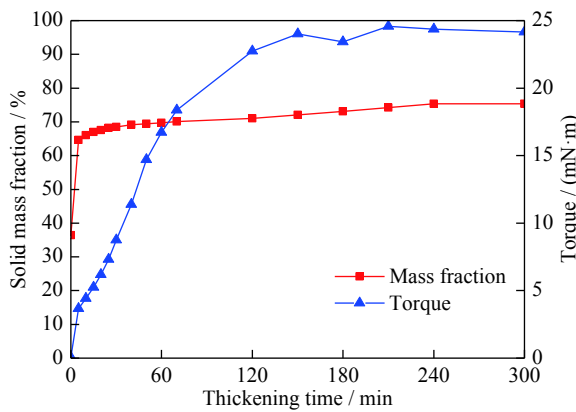


Fig. 8. Simultaneous evolution of solid mass fraction and torque at various thickening times.

With an increase in the solid mass fraction, the rake torque rose, rapidly at first and then gently (Fig. 8). Finally, when the solid mass fraction was constant, the torque was also almost unchanged. Furthermore, the relationship between the solid mass fraction and the torque is illustrated in Fig. 9, and the regression equation is given as follows:

$$y = 23710x^{20.614} \tag{4}$$

where y represents torque, mN·m; and x represents solid mass fraction. The multiple correlation coefficient R^2 is 0.9468, which indicates a good correlation between the torque and solid mass fraction of thickened tailings. It should be noted that this relationship between the torque and the solid mass fraction is under a particular condition in this study (in terms of tailings, water, and experimental set). Since the rheology and torque depend on many parameters, such as particle size, solid mass fraction, process water quality, and pH, more experimental factors need to be considered to improve the torque model that applies to different systems.

The relationship can be considered as a power function.

This power function between the torque and the solid mass fraction is comparable to the rake torque model or yield stress and solid mass fraction relationship proposed in other studies [32,41–43]. Therefore, the evolutionary trend of torque in Fig. 9 is reasonable, due to the linear relationship between torque and yield/shear stress.

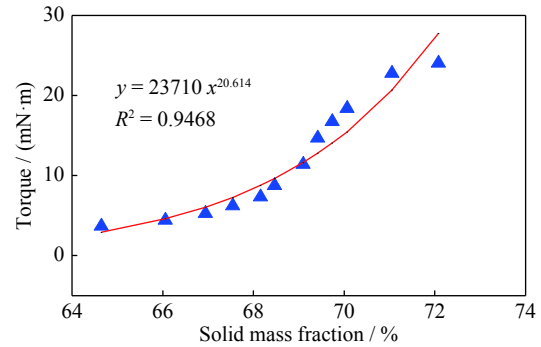


Fig. 9. Relationship between the solid mass fraction and torque and the regression equation.

3.4. Implication for the DCT operation and design

The correlation between the torque and the solid mass fraction offers certain insights for the DCT design and operation:

First, the DCT torque gradually increased during feeding. The torque at the end of the feeding was 1/6 of the torque during smooth operation; this implies that in the early stage of the DCT feeding, there is no need to worry about the rake blockage phenomenon.

Second, in the stage of continuous thickening, the rake torque increased rapidly because of the increase in the solid mass fraction of underflow. During this process, the DCT was fed continuously without underflow discharging.

Third, when the machine was restarted after 5 min shutdown, the rake torque was 1.21 times that under normal smooth running; when the machine was shut down again and restarted after 30 min, the rake torque rose to 1.75 times that under the normal operation. Upon a quick restart after a third shutdown, the torque was 2.3 times that under smooth running, and after a set of data was read, the rake stopped rotating, and a rake blockage occurred. It can be seen that the longer the cumulative downtime, the greater the torque required for the restart. However, as the thickening time and solid mass fraction reached a high level, the rake blockage occurred and the device could not be restarted after the third sudden stop. Therefore, it is recommended that the mud level of the DCT be kept low by stopping the tailings feeding when the underground goaf is not being filled, to avoid restarting or rake blockage because of sudden power failures. In addition, when a power failure occurs, power should be quickly restored to enable the DCT restart early enough, or the internal

slurry in the DCT should be emptied in time to prevent the hardening of the tailings slurry, which will make the DCT fail to restart.

Furthermore, the 30-min restart torque value of this experiment was 1.75 times the torque value under smooth running. Therefore, measures such as underflow flow adjustment, mud height adjustment, and high and low circulation are required to reduce the torque value within the safe range. In the DCT design process, the torque in the tailings thickening process can be measured according to the experimental method presented in this article. Then, the actual DCT torque is similarly estimated, considering the relevant transmission conversion and the safety factor.

4. Conclusions

This study aimed to further clarify the tailings dewatering performance and torque evolution by monitoring the shear stress and torque using a rheometer with a self-made rake. Also, guidance for the DCT operation and design is provided. The main conclusions derived from this study are summarized as follows.

(1) The results of dynamic dewatering tests indicate that the dewatering performance of the total tailings was greatly improved to a solid mass fraction of 75.33% in 4 h, which was 13.64% higher than the limit solid mass fraction of static sedimentation (66.29%).

(2) The tailings thickening process could be divided into three stages: the rapid torque growth period (0–60 min), damping torque growth period (60–120 min), and constant torque thickening zone (after 120 min).

(3) The restart torque after a 5 min shutdown was 1.21 times that under the smooth running before the shutdown; the restart torque after a 30 min shutdown was 1.75 times that under the smooth running; In both the cases of the 5 min shutdown and the subsequent 30 min shutdown, the torque returned to the normal operation value within 2 min; however, when the machine was stopped a third time and restarted quickly (shutdown for 1 min), the rake did not rotate; therefore, the rake blockage phenomenon occurred.

(4) The simultaneous evolution of solid mass fraction and torque at various thickening times was studied. With an increase in the solid mass fraction, the rake torque rose rapidly at first and then gently. The relationship between the solid mass fraction and torque followed a power function, which indicates that the solid mass fraction of thickened tailings can be predicted by the torque evolution.

Acknowledgements

This work was financially supported by the National Natural Science Foundation of China (Nos. 51804015 and 51834001) and the Fundamental Research Funds for the

Central Universities (No. FRF-TP-17-024A1).

References

- [1] C.C. Qi and A. Fourie, Cemented paste backfill for mineral tailings management: Review and future perspectives, *Miner. Eng.*, 144(2019), art. No. 106025.
- [2] S.H. Yin, Y.J. Shao, A.X. Wu, H.J. Wang, X.H. Liu, and Y. Wang, A systematic review of paste technology in metal mines for cleaner production in China, *J. Clean. Prod.*, 247(2020), art. No. 119590.
- [3] D. Wu, R.K. Zhao, C.W. Xie, and S. Liu, Effect of curing humidity on performance of cemented paste back fill, *Int. J. Miner. Metall. Mater.*, 27(2020), No. 8, p. 1046.
- [4] D.L. Wang, Q.L. Zhang, Q.S. Chen, C.C. Qi, Y. Feng, and C.C. Xiao, Temperature variation characteristics in flocculation settlement of tailings and its mechanism, *Int. J. Miner. Metall. Mater.*, 27(2020), No. 11, p. 1438.
- [5] T. du Toit and M. Crozier, Khumani iron ore mine paste disposal and water recovery system, *J. South. Afr. Inst. Min. Metall.*, 112(2012), No. 3, p. 211.
- [6] H.Z. Jiao, S.F. Wang, Y.X. Yang, and X.M. Chen, Water recovery improvement by shearing of gravity-thickened tailings for cemented paste backfill, *J. Clean. Prod.*, 245(2020), art. No. 118882.
- [7] M. Unesi, M. Noaparast, S.Z. Shafaei, and E. Jorjani, Modeling the effects of ore properties on water recovery in the thickening process, *Int. J. Miner. Metall. Mater.*, 21(2014), No. 9, p. 851.
- [8] M. Edraki, T. Baumgartl, E. Manlapig, D. Bradshaw, D.M. Franks, and C.J. Moran, Designing mine tailings for better environmental, social and economic outcomes: A review of alternative approaches, *J. Clean. Prod.*, 84(2014), p. 411.
- [9] A.X. Wu, Z.E. Ruan, R. Bürger, S.H.Y. J.D. Wang, and Y. Wang, Optimization of flocculation and settling parameters of tailings slurry by response surface methodology, *Miner. Eng.*, 156(2020), art. No. 106488.
- [10] H.Z. Jiao, S.F. Wang, A.X. Wu, H.M. Shen, and J.D. Wang, Cementitious property of NaAlO₂-activated Ge slag as cement supplement, *Int. J. Miner. Metall. Mater.*, 26(2019), No. 12, p. 1594.
- [11] A.X. Wu, Z.E. Ruan, C.P. Li, S.Y. Wang, Y.M. Wang, and J.D. Wang, Numerical study of flocculation settling and thickening of whole-tailings in deep cone thickener using CFD approach, *J. Cent. South Univ.*, 26(2019), No. 3, p. 711.
- [12] R. Jewell and A.B. Fourie, *Paste and Thickened Tailings: A Guide*, Australian Centre for Geomechanics, Perth, 2012.
- [13] F. Concha and R. Bürger, A century of research in sedimentation and thickening, *KONA Powder Part. J.*, 20(2002), p. 38.
- [14] M. Tanguay, P. Fawell, and S. Adkins, Modelling the impact of two different flocculants on the performance of a thickener feedwell, *Appl. Math. Modell.*, 38(2014), No. 17-18, p. 4262.
- [15] A. Farkish and M. Fall, Rapid dewatering of oil sand mature fine tailings using super absorbent polymer (SAP), *Miner. Eng.*, 50-51(2013), p. 38.
- [16] S. Wang, X.J. Wang, Q.S. Chen, X.P. Song, J.C. Qin, and Y.X. Ke, Influence of coarse tailings on flocculation settlement, *Int. J. Miner. Metall. Mater.*, 27(2020), No. 8, p. 1065.
- [17] A.T. Owen, T.V. Nguyen, and P.D. Fawell, The effect of flocculant solution transport and addition conditions on feedwell performance in gravity thickeners, *Int. J. Miner. Process.*, 93(2009), No. 2, p. 115.
- [18] T.V. Nguyen, J.B. Farrow, J. Smith, and P.D. Fawell, Design

- and development of a novel thickener feedwell using computational fluid dynamics, *J. South. Afr. Inst. Min. Metall.*, 112(2012), No. 11, p. 939.
- [19] R.B. White, I.D. Šutalo, and T. Nguyen, Fluid flow in thickener feedwell models, *Miner. Eng.*, 16(2003), No. 2, p. 145.
- [20] M. Ebrahimzadeh Gheshlaghi, A. Soltani Goharrizi, and A. Aghajani Shahrivar, Simulation of a semi-industrial pilot plant thickener using CFD approach, *Int. J. Min. Sci. Technol.*, 23(2013), No. 1, p. 63.
- [21] F. Concha, J. P. Segovia, S. Vergara, A. Pereira, E. Elorza, P. Leonelli, and F. Betancourt, Audit industrial thickeners with new on-line instrumentation, *Powder. Technol.*, 314(2017), p. 680.
- [22] A.X. Wu, Y. Wang, and H.J. Wang, Effect of rake rod number and arrangement on tailings thickening performance, *J. Cent. South Univ.*, 45(2014), No. 1, p. 244.
- [23] J. Du, R.A. Pushkarova, and R.S.C. Smart, A cryo-SEM study of aggregate and floc structure changes during clay settling and raking processes, *Int. J. Miner. Process. J.*, 93(2009), No. 1, p. 66.
- [24] G. Huang, J.T. Liu, L.J. Wang, and Z.H. Song, Flow field simulation of agitating tank and fine coal conditioning, *Int. J. Miner. Process.*, 148(2016), p. 116.
- [25] Z.E. Ruan, C.P. Li, and C. Shi, Numerical simulation of flocculation and settling behavior of whole-tailings particles in deep-cone thickener, *J. Cent. South Univ.*, 23(2016), No. 3, p. 740.
- [26] M. Rudman, K. Simic, D.A. Paterson, P. Strode, A. Brent, and I.D. Šutalo, Raking in gravity thickeners, *Int. J. Miner. Process.*, 86(2008), No. 1-4, p. 114.
- [27] Z.E. Ruan, Y. Wang, A.X. Wu, S.H. Yin, and F. Jin, A theoretical model for the rake blockage mitigation in deep cone thickener: A case study of lead-zinc mine in China, *Math. Probl. Eng.*, 2019(2019), art. No. 2130617.
- [28] R. Kahane, T. Nguyen, and M.P. Schwarz, CFD modelling of thickeners at Worsley Alumina Pty Ltd, *Appl. Math. Modell.*, 26(2002), No. 2, p. 281.
- [29] M. Rudman, D.A. Paterson, and K. Simic, Efficiency of raking in gravity thickeners, *Int. J. Miner. Process.*, 95(2010), No. 1-4, p. 30.
- [30] H. Li, H.J. Wang, A.X. Wu, H.Z. Jiao, and X.H. Liu, Pressure rake analysis of deep cone thickeners based on tailings' settlement and rheological characteristics, *J. Univ. Sci. Technol. Beijing*, 35(2013), No. 12, p. 1553.
- [31] H.J. Wang, X. Zhou, A.X. Wu, Y.M. Wang, and L.H. Yang, Mathematical model and factors of paste thickener rake torque, *Chin. J. Eng.*, 40(2018), No. 6, p. 673.
- [32] C.K. Tan, J. Bao, and G. Bickert, A study on model predictive control in paste thickeners with rake torque constraint, *Miner. Eng.*, 105(2017), p. 52.
- [33] H. J. Wang, Q. R. Chen, A. X. Wu, Y. G. Zhai, and X. P. Zhang, Study on the thickening properties of unclassified tailings and its application to thickener design, *J. Univ. Sci. Technol. Beijing*, 33(2011), No. 6, p. 676.
- [34] F.N. Shi and X.F. Zheng, The rheology of flotation froths, *Int. J. Miner. Process.*, 69(2003), No. 1-4, p. 115.
- [35] A.M. Salam, B. Örmeci, and P.H. Simms, Determination of the optimum polymer dose for dewatering of oil sands tailings using UV-vis spectrophotometry, *J. Pet. Sci. Eng.*, 147(2016), p. 68.
- [36] Y. Wang, A.X. Wu, H.J. Wang, S.Z. Liu, and B. Zhou, Influence mechanism of flocculant dosage on tailings thickening, *J. Univ. Sci. Technol. Beijing*, 35(2013), No. 11, p. 1419.
- [37] Y. Wang, A.X. Wu, H.J. Wang, and B. Zhou, Dynamic thickening characteristics and mathematical model of total tailings, *Rock Soil Mech.*, 35(2014), Suppl. 2, p. 168.
- [38] H.J. Wang, Y. Wang, A.X. Wu, B. Zhou, P. Yang, S.F. Yu, and N.B. Peng, Dynamic compaction and static compaction mechanism of fine unclassified tailings, *J. Univ. Sci. Technol. Beijing*, 35(2013), No. 5, p. 566.
- [39] S. Mizani and P. Simms, Method-dependent variation of yield stress in a thickened gold tailings explained using a structure based viscosity model, *Miner. Eng.*, 98(2016), p. 40.
- [40] S. Mizani, P. Simms, and W. Wilson, Rheology for deposition control of polymer-amended oil sands tailings, *Rheol. Acta*, 56(2017), No. 7-8, p. 623.
- [41] L. Huynh, D.A. Beattie, D. Fornasiero, and J. Ralston, Effect of polyphosphate and naphthalene sulfonate formaldehyde condensate on the rheological properties of dewatered tailings and cemented paste backfill, *Miner. Eng.*, 19(2006), No. 1, p. 28.
- [42] S. Lim, K.H. Ahn, S.J. Lee, A. Kumar, N. Duan, X. Sun, S.P. Usher, and P.J. Scales, Yield and flow measurement of fine and coarse binary particulate mineral slurries, *Int. J. Miner. Process.*, 119(2013), p. 6.
- [43] A.X. Wu, Y. Wang, and H.J. Wang, Estimation model for yield stress of fresh uncemented thickened tailings: Coupled effects of true solid density, bulk density, and solid concentration, *Int. J. Miner. Process.*, 143(2015), p. 117.